Biochemical and Histopathological Evaluation of Graphene Oxide in Sprague-Dawley Rats

AK Patlolla[1,2,*], **J Rondalph**[3], and **PB Tchounwou**[1,2]

[1]NIH-RCMI Center for Environmental Health, College of Science Engineering and Technology, Jackson State University, USA

[2]Department of Biology CSET, Jackson State University, USA

[3]Jackson Public School, USA

Abstract

Graphene and its derivatives are promising material for important biomedical applications due to their versatility. A detailed comprehensive study of the toxicity of these materials is required in context with the prospective use in biological setting. We investigated toxicity of Graphene Oxide (GO) in rats following exposure with respect to hepatotoxicity and oxidative stress biomarkers. Four groups of five male rats were orally administered GOs, once a day for five days, with doses of 10, 20 and 40mg/Kg GO. A control group consisted of five rats. Blood and liver were collected 24h after the last treatment following standard protocols. GO's exposure increased induction of Reactive Oxygen Species (ROS), activities of liver enzymes (Alanine ALT, Aspartate AST, Alkaline Phosphates ALP), concentration of Lipid Hydro Peroxide (LHP) and morphological alterations of liver tissue in exposed groups compared to control. The highest two doses, 20 and 40mg/kg, showed statistically significant ($p<0.05$) increases in the induction of ROS, activities of ALT, ALP, LHP concentration, and morphological alterations of liver tissue compared to control. However, AST activity showed no effect. The results of this study demonstrate that GO may be hepatotoxic, and its toxicity might be mediated through oxidative stress.

Keywords

Graphene Oxide; Reactive Oxygen Species; Alanine Aminotransferases; Aspartate Aminotransferases; Lipid Hydroperoxide; Sprague-Dawley Rats

Introduction

Recently, graphene and graphene-related materials are considered the future of advanced nanomaterials owing to their exemplary properties and to their applications in biotechnology

and medicine. However, the information about their potential toxicity is limited, causing concern regarding potential health hazards, similar to e.g. Carbon Nano Tubes (CNT), despite the quite different 2-dimensional structure and large lateral size [1].

Graphene oxide is a single-atomic-layered nanomaterial, which is obtained by the oxidation of graphite crystals, which are inexpensive and abundant. After oxidation, the hydroxyl and carboxyl groups are formed in GO and, when conjugated, such particles can be effectively dispersed in aqueous solutions [2]. It is dispersible in water, and as a result is easy to process. Most importantly, it can be converted back into graphene.

GO can be used for the immobilization of various biomolecules, due to its large surface area and also it has been considered as a candidate for drug-delivery [1–3]. The biological applications of GO have not been well studied, however, its biocompatibility was studied successfully in fibroblast cells (L-929) [4] and it has been used as a carrier for controlled drug-delivery and the release of anticancer drugs [5,6]. In previous reports GO was shown to induce oxidative stress in neural pheochromocytoma-derived PC12 cells [7]. Liu et al. [1,3] study, reported PEGylated nano-GO could be used to deliver water insoluble anticancer drugs without any toxicity. Various studies have reported the antibacterial activity of graphene-based nanomaterials [8–12]. Chronic toxicity and lung granuloma death was reported in mice after GO administration [13]. In other reports [14,15]. Dose-dependent pulmonary toxicity, granulomatous lesions, pulmonary edema fibrosis and inflammatory cell infiltrations were also found after GO administration. Schinwald et al. [16] reported a pulmonary inflammatory response in rats after BSA-capped graphene administration. The number of *in vivo* studies based on tissue distribution and excretion of graphene is gradually increasing.

The proposed mechanism involved in toxicity of nanomaterials is its ability to interact with biological tissues and generate reactive oxygen species [17]. They are well known to play both deleterious and a beneficial role in biological interactions. Mostly, the harmful effects of ROS on the cell are often damage to DNA, oxidation of polydesatured fatty acids in lipid (lipid peroxidation) oxidations of amino acids in proteins and oxidatively inactivate specific enzymes by oxidation of co-factors. Many different forms of fine, ultrafine and nanoscale particles, to be associated with minimal metal contamination have been shown to increase the generation of ROS [18,19].

The oxidative catabolism of polyunsaturated fatty acids, Lipid Peroxidation (LPO), is widely accepted as a general mechanism for cellular injury and death [20,21]. Free radicals and LPO generation are complex and deleterious processes that are closely related to toxicity [3,22]. LOP has been implicated in diverse pathological conditions. The extension of the oxidative catabolism of lipid membranes can be evaluated by several endpoints, but the most widely used method is the quantification of Lipid Hydroperoxide (LHP), one of the stable aldehydic products of lipoperoxidation, present in biological samples [23]. Liver is an important organ in vertebrates including humans, its plays a significant chemical metabolism. The methods normally employed for the detection of hepatotoxicity vary with the circumstances of their use. *In vivo* studies are essential to demonstrate a toxic agent that has in fact a demonstrable adverse effect on the liver in a setting of physiological

significance. Biochemically, serum enzyme analyses have become the standard measure of hepatotoxicity during the past 25 years [24].

This study assesses the effects, after oral administration of GO on ROS induction and various hepatotoxicity markers in the rat model. The question of the health effects of GOs is quite acute and this study brings new data in a field where the largest proportion of publications have been conducted with pulmonary models. Few studies that involves GO focus on the possible pulmonary distress causing excessive inflammation [14]. Pulmonary edema and lung granulomas formation [13,25]. There is a limited knowledge relating to their environmental toxicity and biological safety profile. Extensive testing is now deemed essential for graphene-based materials to assess their biological safety profile. Therefore the results presented here are of importance for health risk assessment.

Material and Methods

Chemicals and reagents

Graphene oxide (40nm diameter) was purchased from Graphene Supermarket (Reading, MA, USA) and was dissolved in water. Xylene, ethyl alcohol, paraffin wax, hematoxylin-eosin stain, Diagnostic enzyme assay kits were obtained from Sigma, (St. Louis MO, USA). Diagnostic kit for Lipid peroxidation assays were purchased from Calbiochem (La, Jolla, CA, USA).

Animal maintenance

Healthy adult male Sprague-Dawley rats (8–10 weeks of age, with average Body Weight (BW) of 125±2g) were used in this study. They were obtained from Harlan-Sprague-Dawley Breeding Laboratories in Indianapolis, Indiana, USA. The rats were randomly selected and housed in polycarbonate cages (18.88 in x7.25 in x3.76 in) (three rats per cage) with steel wire tops and corn-cob bedding. They were maintained in a controlled atmosphere with a cyclic 12h dark/12h light cycle, a temperature of 22 ±2°C and 50–70% humidity and also with free access to pelleted feed (oval normal diet with complete balanced nutritional value for biomedical research) and fresh tap water. The rats were allowed to acclimate for 10 days before treatment.

Doses of graphene oxide

Groups of five rats each were treated with three doses of Graphene Oxide (GO). GO was diluted with deionized water, and orally administered using feeding needles to the rats at the doses of 10, 20, 40mg/Kg BW. Each rat received a total of five doses at 24h intervals. Deionized water was used as negative control and was administered in the same manner as in the treatment groups.

All animal experiments were performed in compliance with the national guidelines for the care and use of experimental animals. Procedures involving the animals and their care conformed to the institutional guidelines, in compliance with national and international laws and guidelines for the use of animals in biomedical research [26].

The size of GO was characterized using Transmission Electron Microscopy (TEM) (Figure 1). The GO was homogeneously dispersed in water. A drop of the homogeneous suspension on a copper grid with a lacey carbon film and allowed to be air-dried. Images were collected using a field emission JEOL-JEM-2100F, TEM, operating at 200KV (JEOL, Tokyo, Japan).

Nanostructure size and zeta potential were measured in Deionized Water (DI water) using a Nano Zetasizer (Malvern, Worcestershire, UK) (Figure 2). Briefly, the nanoparticle samples were measured after dilution of a GO stock solution of $50\mu g$/ml in water. These dilutions were vortexed and sonicated for 5min to provide a homogenous dispersion. For the size measurement, 1ml of the diluted GOs dispersion was transferred to a 1cm2 cuvette for dynamic size measurement. For zeta potential measurement, a Malvern zeta potential cell was washed 3–4 times with ultrapure water followed by transferring $850\mu l$ of diluted GOs dispersion to this cell to measure the zeta potential. To assure the quality of the data the concentration of the samples and experimental methods were optimized. Sixty nm NIST standard gold nanoparticles was used in the validation of the instrument. Both size and zeta potential were measured at least three times. The data was calculated as the average size or zeta potential of GO's.

Preparation of homogenates

At the end 5 days exposure to GOs, the liver was excised under anesthesia. The organs were washed thoroughly in ice-cold physiological saline and weighed. 10% homogenate of each tissue was prepared separately in 0.05M phosphate buffer (pH 7.4) containing 0.1mM EDTA using a motor driven Teflon-pestle homogenizer (Fischer), followed by sonication (Branson Sonifer), and centrifugation at 500xg for 10 min at 4°C. The supernatant was decanted and centrifuged at 2000xg for 60min at 40C. The cellular fraction obtained was called 'homogenate' and was used for the assays.

Reactive Oxygen Species (ROS) detection

DCFH-DA method with slight modification was used to quantify ROS production [27]. It is based on the ROS-dependent oxidation of DCFH-DA to DCF. An aliquot of liver homogenates from each exposed group and controls were centrifuged at 1000xg for 10min (4°C). The supernatants were re-centrifuged at 1000xg for 20min at 4°C, and then the pellet was re-suspended. The DCFH-DA solution with the final concentration of $50\mu M$ and re-suspension were incubated for 30min at 37°C. Fluorescence of the samples was monitored at an excitation wavelength of 485nm and an emission wavelength of 538nm after 5 days. The positive control, hydrogen peroxide (30% H_2O_2), was used to assess the reactivity of the probe.
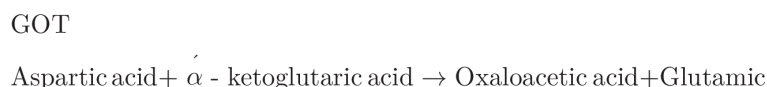
Serum biochemical analysis

Following anesthetization, blood specimens were immediately collected using heparinized syringes, and transferred into polypropylene tubes. Each sample was allowed to clot for a minimum of 30min (maximum 60min). After clotting, the sample was centrifuged at 750xg for 10min. The serum then was pipetted from the cellular elements (erythrocytes, platelets, leucocytes) and transferred to an acid-washed polypropylene tube, properly labeled, and stored at 4°C until ready for analysis. The activities of certain liver enzymes such as alanine

(GPT) and aspartate (GOT) aminotransferases, alkaline (ALP) phosphates in the serum samples were determined using colorimetric assay kits from Sigma (St. Louis MO, USA).
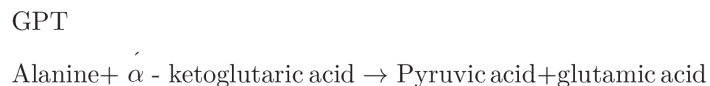
Enzyme analysis

Serum aminotransferases—A method by Reitman and Franke [28] was followed to determine the activities of alanine or Glutamate Pyruvate Transaminase (ALT/GPT) and aspartate or Glutamate Oxaloacetate Transaminase (AST/GOT) in serum. Human serum contains many different transaminases. The two most commonly determined are ALT/GPT and AST/GOT. These enzymes catalyze transfer of alpha amino groups from specific amino acids to Alpha-Ketoglutaric Acid [AKG] to yield glutamic acid and oxaloacetic or pyruvic acid. The keto acids are then determined colorimetrically after their reaction 2, 4-Dinitrophenyl Hydrazine [DNP]. The absorbance of the resulting color is then measured at wavelength of approximately 505nm to take advantage in the absorption that exists between the hydrazones of AKG and the hydrazones of oxaloacetic acid or pyruvic acid.

The reaction for GOT is as follows:

$$\text{Aspartic acid} + \alpha\text{-ketoglutaric acid} \xrightarrow{\text{GOT}} \text{Oxaloacetic acid} + \text{Glutamic}$$

The reaction for GPT is as follows:

$$\text{Alanine} + \alpha\text{-ketoglutaric acid} \xrightarrow{\text{GPT}} \text{Pyruvic acid} + \text{glutamic acid}$$

Alkaline phosphatases—To determine the activity of alkaline phosphatase in serum a method by Kay et al., [29] was followed; it was measured using a Diagnostic kit from Sigma (St. Louis MO, USA). Alkaline phosphatase is also known as orthhophosphoric monoester phosphohydrolase, ALP. It is a prototype of those enzymes that reflect pathological reductions in bile flow. This enzyme has been extensively employed in experimentally induced hepatic dysfunction. Alkaline phosphatase refers, not to a single enzyme, but to a family of enzymes with different physico-chemical properties and broad overlapping substrate specificities.

The procedure for alkaline phosphatase depends upon the hydrolysis of p-nitrophenyl phosphate by the enzyme, yielding p-nitrophenol and inorganic phosphate. When made alkaline, p-nitrophenol is converted to a yellow complex readily measured at 400–420nm. The intensity of color formed is proportional to phosphatase activity.

The reaction for ALP is as follows:

$$\text{Orthophosphoric monoester} + H_2O \xrightarrow{\text{ALP}} \text{alcohol} + H_3PO_4$$

Lipid hydro peroxidation assay—The tissues were homogenized (1:8, w/v) in cold HPLC-grade water. Five hundred microliter (500μl) of the each tissue homogenate was taken in a glass test tube and equal volume of Calbiochem supplied Extract R saturated methanol was added. The mixture was vortexed for few minutes and 1ml of cold deoxygenated chloroform was added to the sample mixture, vortexed it thoroughly. The mixture was centrifuged at 1500xg for 5min at 0°C (Beckman XL-100K, USA) and bottom chloroform layer was collected. Five hundred μl of the bottom chloroform was mixed with 450μl of chloroform: methanol (2:1) mixture and 50μl of Calbiochem supplied chromogen (thiocyanate ion). Then the mixture was incubated for 5min and the absorbance of each sample was recorded at 500nm wavelength using spectrophotometer (2800 Unico spectrophotometer USA). This method directly measures the lipid hydro-peroxides utilizing redox reactions with ferrous ions, the produced hydroperoxides are highly unstable and react readily with ferrous ions to produce ferric ions. The produced ferric ions were detected using thiocyanate ion as chromogen. Calbiochem supplied lipid hydroperoxides solution was used as reference standard.

Histopathological analysis—Liver was surgically removed from mice under diethyl ether anesthesia. Portions of liver were taken and washed with ice-cold normal saline (0.9% Nacl) and 20mM EDTA to remove blood, cut into small pieces, and fixed immediately in 10 percent phosphate-buffered formalin for 48hrs. The tissues were then transferred to 70% ethyl alcohol and stored until processed. The tissue specimens (liver) were processed, embedded in paraffin, sectioned at 0.1μm, and stained with Hematoxylin and Eosin (H & E) for histological examination under a light microscope. The extent of tissue injury was estimated semi-quantitatively and lesions scored as multi-focal fibrosis/necrosis. At least 10 slides of each sample were scored for liver histology. The liver morphology scored as follows: 0=normal, 1=mild cellular disruption in less than 25% of field area, 2=moderate cellular disruption and hepato cellular vacuolation greater than 50% of field area, 3=extensive cell disruption, hepato cellular vacuolation, necrosis, and condensed nuclei (pycknotic) of hepatocytes in greater than 50% of field area.

Statistical analysis

Statistical analysis was performed with SAS 9.1 software for Windows XP. Data was presented as Means ± SDs. One-Way Analysis Of Variance (ANOVA) with p-values less than 0.05 were considered as statistically significant.

Results

Nanomaterial characterization

Morphology, diameter, tendency of aggregation and cellular distribution of nanoparticles were characterized by using Transmission Electron Microscope (TEM) (JEOL-1011). Mainly spherical shaped Graphene Oxide (GO) were observed (Figure 1). To understand the state of dispersion of the particles when placed into deionized water (DI water), the GOs sample was analyzed by Dynamic Light Scattering (DLS) (Figure 2). The results from DLS showed agglomeration of GOs more than its primary size (40nm), and the zeta potential

value of GOs was shown to be −33.2mV. A solution is considered stable if the zeta potential value is more negative than −30mV or more positive than 30 mV (Figure 2).

ROS detection

The administration of GO to rats significantly enhanced the ROS level at four tested doses as compared to the control animals. (Figure 3) summarizes the detection of intracellular production of ROS in rats exposed to GO and controls. The results yielded fluorescence of 425.04+2.75, 534.20+5.84, 885.01+5.47, and 946.71+10.70 for control, 10, 20, and 40 mg/Kg GOs respectively (Figure 3).

Enzyme analysis

Alanine aminotransferase and aspartate aminotransferase—Figure 4 presents the experimental data obtained from the analysis of alanine aminotansferases (ALT/GPT). The results yielded optical density readings of 79.4+0.01, 127+0.03, 236+0.01, and 271+0.05, for 0, 10, 20 and 40 mg/kg Bwt. of GO respectively were observed. As shown in this figure there was an increase in the activity of alanine (ALT/GPT) in the serum of Sprague-Dawley rats. However, the highest doses 20 and 40 mg/kg were found to show statistically significant effect in elevating the activity of ALT/GPT when compared to control.

Graphene oxide exposure resulted in elevating the activity of AST/GOT. However, there was no statistically significant effect in the activity of exposed rats compared to control. Optical density readings of 199+0.011, 214+ 0.04, 239+0.011, and 233+0.013 for 0, 10, 20 and 40 mg/kg Bwt. of GO respectively was obtained (Figure 4).

Alkaline phosphatases

The activity of alkaline phosphatase exposed to GO is represented in (Figure 5). As shown in the figure there was an increase in the activity of alkaline phosphatases in rats treated with GO compared to control. However, the highest concentrations 20mg/Kg and 40mg/kg were found to show statistically significant effect in elevating the activity. Optical density readings of 1.28+0.019, 1.89+0.032, 4.15+0.019 and 5.28+0.027 for 0, 10, 20 and 40mg/kg Bwt GO respectively was obtained.

Lipid Hydro Peroxides (LPO)

Lipid hydro peroxides assay was performed to determine the hydroperoxides levels in serum of rats exposed to GO and controls. The MDA standard curve is presented in (Figure 6a). The LPO levels of the serum were significantly increased in all the treatment groups compared to the control groups. The LPO levels in serum were 31.7+2.03, 55.8+3.11, 77.1+4.62 and 83.3+4.62μM for 0, 10, 20 and 40mg/kg BWt GO, respectively (Figure 6b).

Histopathological evaluation

Microscopic examination of the control liver had normal structure and compactly arranged hepatocytes. Sinusoids were scattered randomly all over the hepatocytes and the hepatocytes had uniform morphology along with central vein. However, the rats exposed to 10, 20 and 40mg/Kg of GO had remarkable morphological alterations. Hepatocytes disruption and

hepatocellular vacuolation was observed in microscopic examination of 10mg/Kg exposed rat liver. In addition to the 10mg/Kg alterations, pycknotic or karyomegaly (condensed nuclei) of hepatocytes and partial disruption of central vein was observed in 20mg/Kg of GO exposed rat liver. In addition to the above alterations, degeneration of liver (atrophy) and central vein injury was observed in 40mg/Kg GO exposed rat liver. Treated and control rat liver photos were presented in the (Figure 7).

Discussion

Nanomaterials have the potential to cause organ damage throughout the body as they have been shown to enter systemic circulation. Those organs with extensive blood supply such as liver are especially vulnerable [30]. Hepatotoxicity and oxidative stress biomarkers such as induction of ROS, activities of certain liver enzymes (ALT/GPT, AST/GOT and ALP), measurement of lipid hydroperoxide and histopathology of liver tissue in rats exposed to graphene oxide were studied. In the present study, there was a significant increase in the level of ROS in liver homogenate of rats exposed to GO compared to controls. ROS has been implicated in the toxicity of nanomaterials [17,31] by several reports. Their formation with subsequent cellular damage is considered as the molecular mechanism of nanomaterials-induced toxicity.

The liver is a vital organ that is responsible for many biochemical processes in biological systems. It drives a variety of metabolic reactions and synthesizes large number of enzymes. Further, most of the toxic chemicals are metabolized in the liver, a condition that causes a high risk of injury and leads to hepatotoxicity [32]. Liver cells or hepatocytes are easily disintegrated by a variety of factors and harmful products, and accumulation of graphene in the liver cause alterations of hepatic function [33]. Degeneration, inflammation and necrosis caused by hepatocyte damage can lead to an increase in the permeability of cell membrane. Thus AST and ALT are released into the body through the cell membrane and hence their concentration in the blood increases. AST and ALT are indicators of liver damage [32,34]. The results with serum aminotransferases in the present study were found to show an increase in the activity of ALT/GPT and AST/GOT with increasing concentration of GO, however only the highest doses 20 mg/kg and 40 mg/kg were found to show a statistically significant increase in the activity of ALT/GPT compared to control. Aspartate transferases did not show any statistically significant effect in elevating the activity of the enzyme.

In the present study GO significantly increased the activity of ALP enzyme in the serum of treated rats compared to control suggesting possible injuries to the liver tissue. Alkaline Phosphatase (ALP) enzyme, one of the main group of the family of phosphatases [35] is widely used as an indicator of hepatobiliary disease. ALP of the liver is produced by the cells lining the small bile ducts (ductoles) in the liver. If the liver disease is primarily of an obstructive nature (cholestatic) i.e., involving the biliary drainage system, the ALP will be the first and foremost enzyme found to increase and elevation of ALP in the serum is usually indicated in liver damage or impaired hepatic clearance (cholestasis).

To establish the role of oxidative stress as a decisive factor in GO-induced toxicity, the level of lipid hydroperoxides in liver homogenates was performed. Lipid hydroperoxides

(LOOHs) are prominent non-radical intermediates of lipid peroxidation whose identification can often provide valuable mechanistic information, e.g., whether a primary reaction is mediated by singlet oxygen or oxyradicals. The results in the present investigation demonstrated that a dose-dependent increase in the level of lipid hydroperoxides was observed, however, the highest doses of 20 and 40mg/kg bwt GO were found to be statistically significant in increasing the level of lipid hydroperoxidese. Investigation through in vitro studies has revealed that the indirect contact with nanomaterials with mammalian cells causes cytotoxic reactions such as release of ROS and stress followed by cytokine release and inflammation which is primarily in response to ROS [17,33,36]. Further cell damage and lipid peroxidation of cellular membranes are also seen which can result in changes in gene expression involving irregular signaling causing further inflammation [17,33,36]. The toxicity profile of graphene and GO nanoparticles remains elusive, since their characterization and chemical composition are very similar at nanometer scale [37].

Kupffer cells of the liver play an important role in its normal physiology and homeostasis as well as participating in the acute and chronic responses of the liver to toxic compounds. They directly or indirectly are activated by toxic agents resulting in the release of an array of inflammatory mediators, growth factors, and reactive oxygen species. This activation appears to modulate acute hepatocyte injury as well as chronic liver responses including hepatic cancer. The key in understanding the mechanism of liver injury is to understand the role of Kupffer cells play in diverse responses [38].

In our study histopathological evaluation of liver exposed to GO showed remarkable morphological alterations such as hepatocytes disruption, hepatocellular vacuolation, central vein damage, pycknotic or karyomegaly of hepatocytes and necrosis when compared to control. Zhao et al. [30] study has shown the potential distribution of graphene and its derivatives, highlighting the target organs, systems and distribution throughout the body. Graphene can easily enter into lungs via the respiratory system and later distribute themselves in the circulatory system via blood and lymph fluid. Further investigation into the distribution of grapheme has found that the materials can penetrate into the tissues of the heart, spleen, kidney, bone marrow and liver. Although it is most likely that this impairment in hepatotoxicity biomarkers is associated with GO toxicity, further experiments are needed to elucidate the biochemical mechanisms involved.

Conclusion

In summary, short-term and high toxicity in rats exposed to GO's are reported. Serum biochemical changes, ROS induction, increase in the level of LOP and damage to the liver tissue were observed. The proposed main toxicological mechanism is oxidative stress aroused in liver.

There is a limited knowledge relating to their environmental toxicity and biological safety profile. Therefore further toxicological studies *in vivo* have to be developed for evaluating hazards of occupational or environmental exposure to graphene related nanomaterials.

Acknowledgments

References

1. Sun X, Liu Z, Welsher K, Robinson JT, Goodwin A, Zaric S, et al. Nano-Graphene Oxide for Cellular Imaging and Drug Delivery. Nano Res. 2008; 1:203–212. [PubMed: 20216934]

2. Seabra AB, Paula AJ, de Lima R, Alves OL, Duran N. Nanotoxicity of graphene and graphene oxide. Chem Res Toxicol. 2014; 27:159–168. [PubMed: 24422439]

3. Liu Z, Robinson JT, Sun X, Dai H. PEGylated nanographene oxide for delivery of water-insoluble cancer drugs. J Am Chem Soc. 2008; 130:10876–10877. [PubMed: 18661992]

4. Schipper ML, Ratchford NN, Davis CR, Kam NW, Chu P, Liu Z, et al. A pilot toxicology study of single-walled carbon nanotubes in a small sample of mice. Nat Nanotechnol. 2008; 3:216–221. [PubMed: 18654506]

5. Zhang L, Xia J, Zhao Q, Liu L, Zhang Z. Functional graphene oxide as a nanocarrier for controlled loading and targeted delivery of mixed anticancer drugs. Small. 2009; 6:537–544.

6. Yang X, Zhang X, Liu Z, Ma Y, Huang Y, Chen Y. High-Efficiency Loading and Controlled Release of Doxorubicin Hydrochloride on Graphene Oxide. J Phys Chem. 2008; 112:17554–17558.

7. Zhang YB, Ali SF, Dervishi E, Xu Y, Li Z, Casciano D, et al. Cytotoxicity effects of graphene and single-wall carbon nanotubes in neural phaeochromocytoma-derived PC12 cells. ACS Nano. 2010; 4:3181–3186. [PubMed: 20481456]

8. Hu W, Peng C, Luo W, Lv M, Li X, Li D, et al. Graphene-based antibacterial paper. ACS Nano. 2010; 4:4317–4323. [PubMed: 20593851]

9. Akhavan O, Ghaderi E. Toxicity of graphene and graphene oxide nanowalls against bacteria. ACS Nano. 2010; 4:5731–5736. [PubMed: 20925398]

10. Lim HN, Huang NM, Loo CH. Facile preparation of graphene-based chitosan films: Enhanced thermal, mechanical and antibacterial properties. J Non-Cryst Solids. 2012; 358:525–530.

11. Krishnamoorthy K, Veerapandian M, Zhang LH, Yun K, Kim SJ. Antibacterial Efficiency of Graphene Nanosheets against Pathogenic Bacteria via Lipid Peroxidation. J Appl Nanosci. 2012; 116:17280–17287.

12. Mannoor MS, Tao H, Clayton JD, Sengupta A, Kaplan DL, Naik RR, et al. Graphene-based wireless bacteria detection on tooth enamel. Nat Commun. 2012; 3:763. [PubMed: 22453836]

13. Wang K, Ruan J, Song H, Zhang J, Wo Y, Guo S, et al. Biocompatibility of graphene oxide. Nanoscale Res Lett. 2011; 6:8. [PubMed: 27502632]

14. Duch MC, Budinger GR, Liang YT, Soberanes S, Urich D, Chiarella SE, et al. Minimizing oxidation and stable nanoscale dispersion improves the biocompatibility of graphene in the lung. Nano Lett. 2011; 11:5201–5207. [PubMed: 22023654]

15. Zhang S, Yang K, Feng L, Liu Z. *In vitro* and *in vivo* behaviors of dextran functionalized graphene. Carbon. 2011; 49:4040–4049.

16. Schinwald A, Murphy FA, Jones A, MacNee W, Donaldson K. Graphene-based nanoplatelets: a new risk to the respiratory system as a consequence of their unusual aerodynamic properties. ACS Nano. 2012; 6:736–746. [PubMed: 22195731]

17. Nel A, Xia T, Madler L, Li N. Toxic potential of materials at the nanolevel. Science. 2006; 311:622–627. [PubMed: 16456071]

18. Li N, Sioutas C, Cho A, Schmitz D, Misra C, Sempf J, et al. Ultrafine particulate pollutants induce oxidative stress and mitochondrial damage. Envirol Health Perspectives. 2003; 111:455–460.

19. Muller P, Jacobsen NR, Folkmann JK, Danielsen PH, Mikkelsen L, Hemmingsen JG, et al. Role of oxidative damage in toxicity of particulates. Free Radic Res. 2010; 44:1–46. [PubMed: 19886744]

20. Gutteridge JM, Quinlan GJ. Malondialdehyde formation from lipid peroxides in thiobarbituric acid test: The role of lipid radicals, iron salts and metal chelator. J Appl Biochem. 1983; 5:293–299. [PubMed: 6679543]

21. Halliwell B. Oxygen radicals: A commonsense look at their nature and medical importance. Med Biol. 1984; 62:71–77. [PubMed: 6088908]

22. Murray, RK., Granner, DK., Mayes, PA., Rodwell, V. Harper's Biochemistry. 21. International Union of Biochemistry and Molecular Biology; 1988.

23. de Zwart LL, Meerman JH, Commandeur JN, Vermeulen NP. Biomarkers of free radical damage applications in experimental animals and in humans. Free Radic Biol Med. 1999; 26:202–226. [PubMed: 9890655]

24. Zimmerman, S. Diagnostic Enzymology. 1970. Enzymes in hepatic disease.

25. Zhang X, Yin J, Peng C, Hu W, Zhu Z, Li W, et al. Distribution and biocompatibility studies of graphene oxide in mice after intravenous administration. Carbon. 2011; 49:986–995.

26. Giles AR. Guidelines for the use of animals in biomedical research. Thromb Haemost. 1987; 58:1078–1084. [PubMed: 3328319]

27. Lawler JM, Song W, Demaree SR. Hindlimb unloading increases oxidative stress and disrupt antioxidant capacity in skeletal muscle. Free Radic Biol Med. 2003; 35:9–16. [PubMed: 12826251]

28. Reitman S, Frankel S. A colorimetric method for the determination of serum glutamic oxalacetic and glutamic pyruvic transaminases. Am J Clin Pathol. 1957; 28:56–63. [PubMed: 13458125]

29. Kay HD. Plasma phosphatase: I Method of determination. Some properties of the enzyme. J Biol Chem. 1930; 89:235.

30. Zhao X, Liu R. Recent progress and perspectives on the toxicity of carbon nanotubes at organism, organ, cell, and biomacromolecule levels. Environ Int. 2012; 40:244–255.0. [PubMed: 22244841]

31. Nel A. Air pollution-related illness: effects of particles. Science. 2005; 308:804–806. [PubMed: 15879201]

32. Patlolla AK, Berry A, Tchounwou PB. Study of hepatotoxicity and oxidative stress in male Swiss-Webster mice exposed to functionalized multi-walled carbon nanotubes. Mol Cell Biochem. 2011; 358:189–199. [PubMed: 21725842]

33. Oberdorster G, Manard A, Donaldson K, Castranova V, Fitzpatrick J, Ausman K, et al. Principles for characterizing the potential human health effects from exposure to nanomaterials: elements of a screening strategy. Part Fibre Toxicol. 2005; 6:2–8.

34. Patlolla A, McGinnis B, Tchounwou P. Biochemical and histopathological evaluation of functionalized single-walled carbon nanotubes in Swiss-Webster mice. J Appl Toxicol. 2011; 31:75–83. [PubMed: 20737426]

35. Murakami S, Okub K, Tsuji Y, Sakata H, Takahashi T, Kikuchi M, et al. Changes in liver enzymes after surgery in anti-hepatitis C virus-positive Patients. World J Surg. 2004; 28:671–674. [PubMed: 15175902]

36. Oberdörster G, Oberdörster E, Oberdörster J. Nanotoxicology: an emerging discipline evolving from studies of ultrafine particles. Environ Health Perspect. 2005; 113:823–839. [PubMed: 16002369]

37. Nezakati T, Cousins BG, Seifalian AM. Toxicology of chemically modified graphene-based materials for medical applications. Arch Toxicol. 2014; 88:1987–2012. [PubMed: 25234085]

38. Roberts RA, Gane PE, Ju C, Kamendulis LM, Rusn I, Klaunig JE. Role of kupffer cell in mediating hepatic toxicity and carcinogenesis. Toxicol Sci. 2007; 96:2–15. [PubMed: 17122412]
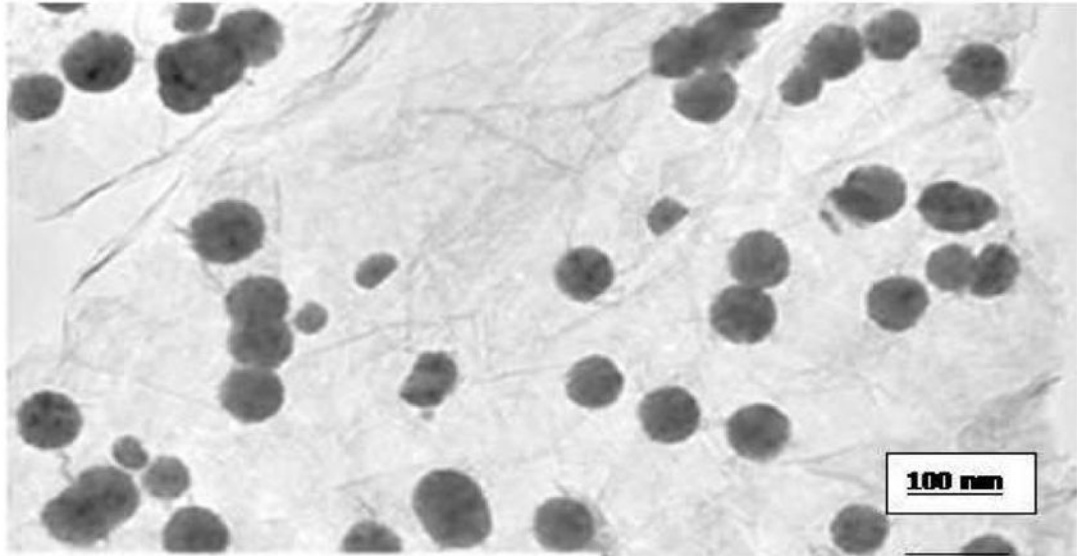
Author Manuscript   Author Manuscript   Author Manuscript   Author Manuscript

Figure 1.
Transmission electron microscope picture of graphene oxide (GO). Diameter size 38nm.
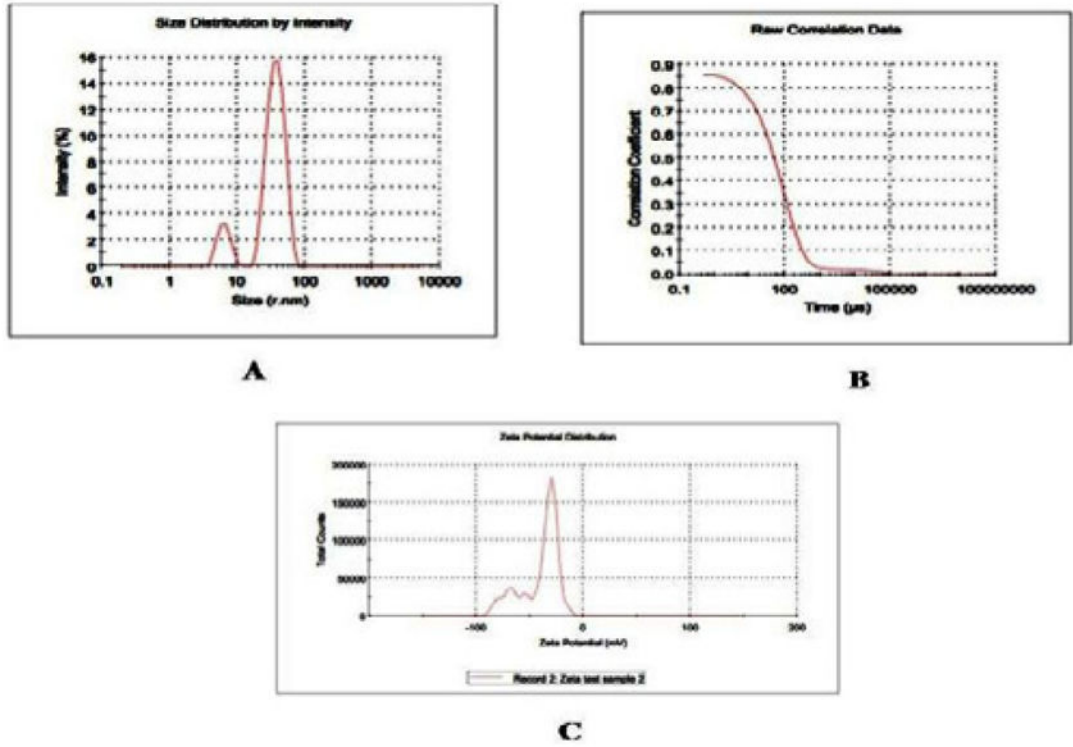
Figure 2.
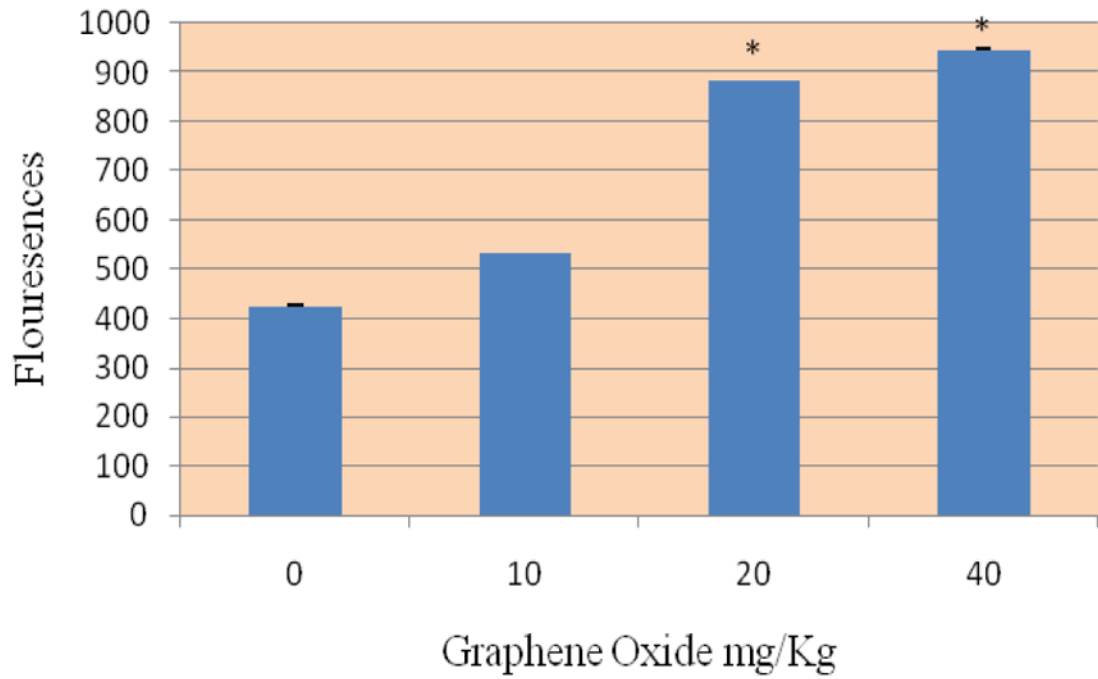A) GO's size by intensity, (B) Raw correlation data (C) Zeta potential.

Figure 3.
Effect of Graphene Oxide on the induction of Reactive Oxygen Species in Sprague-Dawleys rats. Each bar represents mean ± SD of five rats. Values with asterisks were significantly different from control
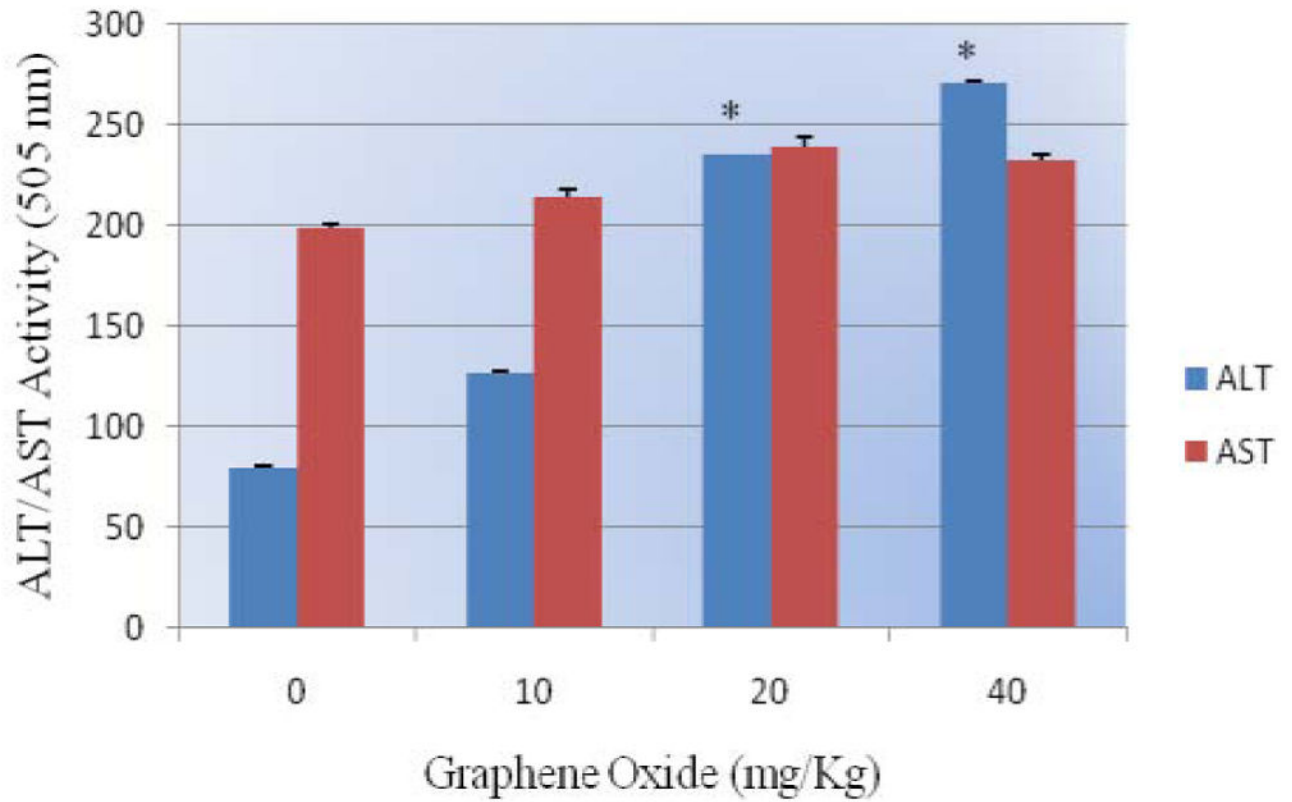
Figure 4.
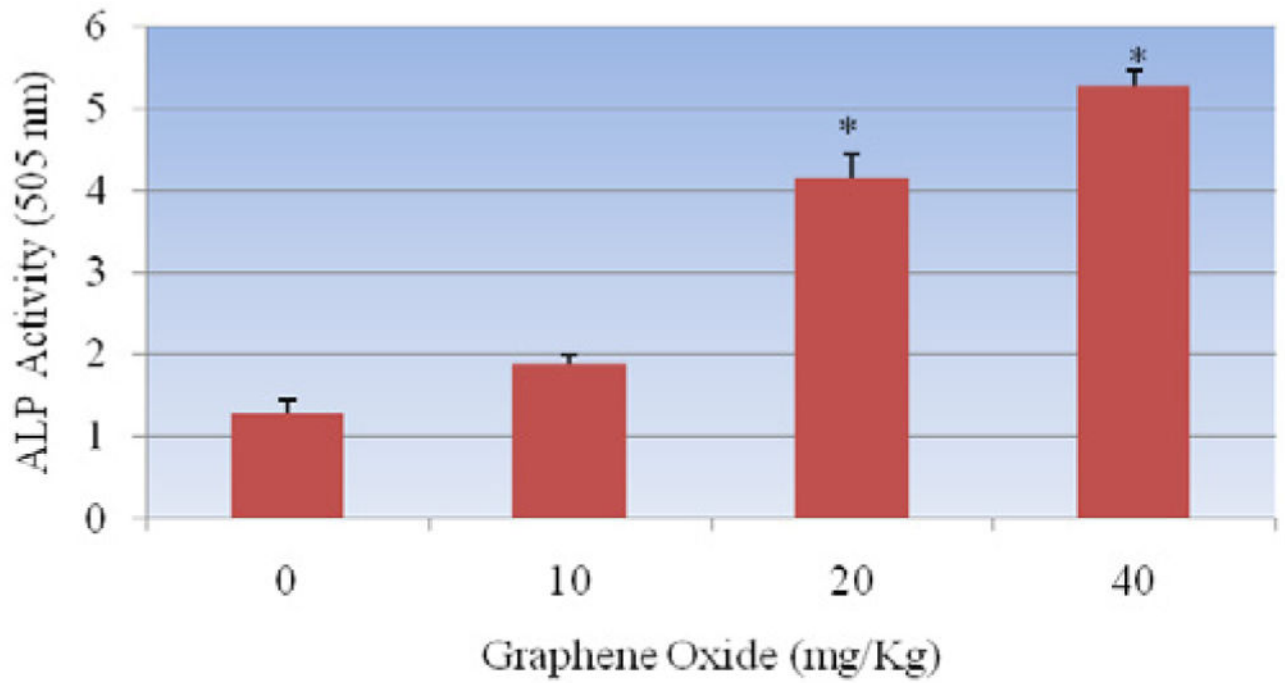Effect of Graphene Oxide on the activity of serum aminotransferases (ALT/AST) in Sprague-Dawleys rats. Each bar represents mean ± SD of five rats. Values with asterisks were significantly different from control.

Figure 5.
Effect of Graphene Oxide on the activity of alkaline phosphatases in Sprague-Dawleys rats. Each bar represents mean ± SD of five rats. Values with asterisks were significantly different from control.
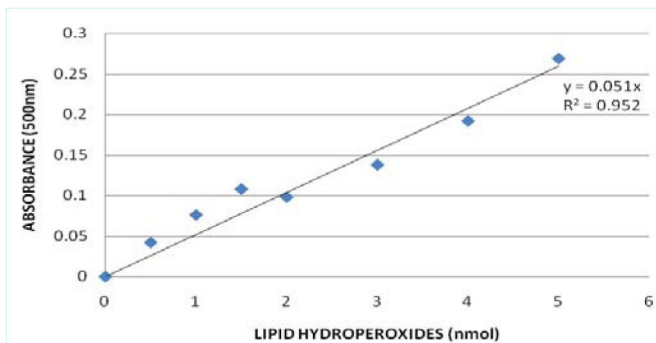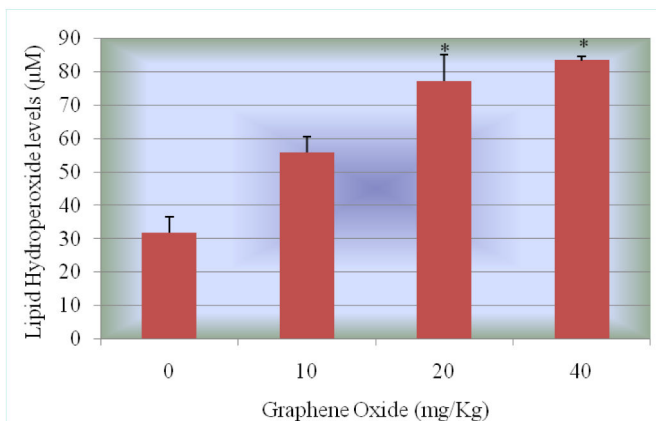
Figure 6a

Figure 6b

Figure 6.

Figure 6a: Standard curve for Lipid Hydro Peroxides (LPO) assay where y-axis represents absorbance at 500nm whereas x-axis represents the concentrations of reference standard (nmol).

Figure 6b: Effect of Graphene Oxide on Lipid Hydro Peroxide. Each bar represents mean ± SD of five rats. Values with asterisks were significantly different from control.
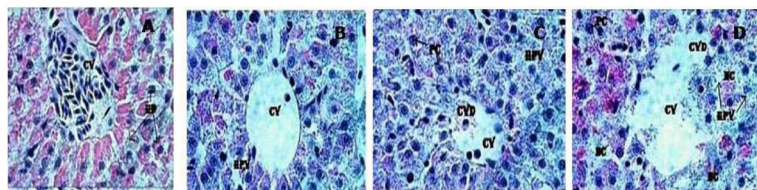
Figure 7.
Histopathological evaluation of Sprague-Dawley rat liver exposed to Graphene Oxide.
A= Control (CV: Central Vein; HP: Hepatocytes), B= 10mg/Kg exposed liver (CV: Central Vein; HPV: Hepato cellular vacuolation), C= 20mg/Kg exposed liver (CV: Central Vein; CVD: Central Vein Damage; HPV: Hepato cellular vacuolation and PC=Pycknotic) and D= 40 mg/Kg exposed liver (CV: Central vein; CVD: Central vein damage, HPV: Hepato cellular vacuolation; NC= Necrosis and PC=Pycknotic). H & E Staining 1000 X.